A stochastic hybrid model for DNA replication incorporating protein mobility dynamics

Jonas Windhager[1,2,4*], Amelia Paine[1*], Patroula Nathanailidou[3], Eve Tasiudi[2], María Rodríguez Martínez[1], Zoi Lygerou[3], John Lygeros[2], and Maria Anna Rapsomaniki[1†]

[1]IBM Research Zurich, Rüschlikon, Switzerland
[2]Dept. of Information Technology and Electrical Engineering, ETH Zurich, Zurich, Switzerland
[3]Dept. of Biology, School of Medicine, University of Patras, Rio, Patras, Greece

[4]Current address: Dept. of Quantitative Biomedicine, University of Zurich, Zurich, Switzerland

[*]These authors contributed equally to this work
[†]Correspondence address: aap@zurich.ibm.com

February 23, 2019

ABSTRACT

DNA replication is a complex process that ensures the maintenance of genetic information. Recently, advancements in chromatin conformation capture techniques have enabled the modeling of DNA replication as a spatio-temporal process. Here, we present a stochastic hybrid model for DNA replication that incorporates protein mobility dynamics and 3D chromatin structure. Performing simulations for three model variations and a broad range of parameter values, we collected about 300,000 *in silico* replication profiles for fission yeast and conducted a parameter sensitivity analysis. We find that the number of firing factors initiating replication is rate-limiting and dominates the time until completion of DNA replication. In support of recent work, we also find that explicitly modeling the recruitment of firing factors by the spindle pole body (SPB) best recapitulates published origin efficiencies, and independently validate these findings *in vivo*. Accounting for probabilistic effects in molecular interactions, we further investigated the replication kinetics inherent to the model and were able to capture known properties of DNA replication. Importantly, we confirm earlier observations that, without further assumptions, the characteristic shape of a function commonly used to describe replication kinetics arises from a rate-limiting number of firing factors in conjunction with their recycling upon replication fork collision. While the model faithfully recapitulates global spatial patterns of replication initiation, additional analysis of spatial concurrence and competition suggests that a uniform binding probability is too simplistic to capture local neighborhood effects in origin firing. In summary, our model provides a framework to realistically simulate DNA replication for a complete eukaryotic genome, and to investigate the relationship between three-dimensional chromatin conformation and DNA replication timing.

1 Introduction

DNA replication is a tightly regulated process that ensures the faithful duplication of the genome before cell division. In eukaryotes, DNA replication initiates from multiple sites along the genome called *replication origins*. During G1 phase, the origin recognition complex (ORC) binds to selected replication origins and recruits additional factors Cdt1, Cdc6 [1, 2], and the helicase MCM2-7 [3, 4]. Together, these molecules form the pre-replicative complex (pre-RC) in a process known as *origin licensing* [5, 6]. After the G1-S transition, a cascade of phosphorylation events, orchestrated by cyclin-dependent kinase (CDK) and Dbf4-dependent kinase (DDK) [7], leads to the binding of additional *firing factors* (e.g., Cdc45, Sl2, Sld3 and GINS [8, 9]) to the pre-RCs of selected origins, forming the pre-initiation complex (pre-IC) [10–12]. These events trigger the helicase activity of the MCM hexamer, the recruitment of DNA polymerases, and the formation of the Cdc45-MCM-GINS (CMG) complex on the pre-ICs [13]. Known as *origin firing* [14], this process is a key decision point in cell cycle progression and concludes with the formation of two sister replisomes (*replication forks*) that move in opposite directions, simultaneously unwinding the DNA and synthesizing a new copy [13, 15]. Recently, a molecular mechanism to ensure the simultaneous activation of replisomes has been proposed, suggesting that firing factors form dimers, which, upon origin activation, monomerize and travel along with both replication forks, before reuniting with neighboring replisomes to release a new firing factor upon fork collision [16].

DNA replication in eukaryotes is a complex and uncertain process: Origin firing is stochastic and replication progression along the genome is unique in every cell cycle and in every cell in a population [17–19]. One aspect of uncertainty regards the base-pair location and sequence characteristics of replication origins *per se*. In fission yeast, replication origins are located in intergenic, nucleosome-depleted regions with high AT content [20–24], while in metazoan genomes the nature of replication origins is more elusive [25, 26]. Another aspect of uncertainty regards both the efficiency (i.e., frequency) and timing of origin firing. The number of pre-ICs is redundant, with only a small subset activated in a single cell cycle and the rest remaining dormant until passive replication [27]. Because selected origins fire in an asynchronous manner, the exact temporal order of origin firing is stochastic. A variety of factors have been shown to influence DNA replication timing [28–30]. Chromosomal context and local chromatin state are major determinants, with euchromatic and pericentromeric regions typically containing early-firing origins, and heterochromatic and subtelomeric regions containing late-firing and/or dormant origins [31]. Last, mammalian genomes are organized in replication timing domains, i.e., large regions containing many synchronously-firing replicons [32, 33].

Recent advancements in chromosome conformation capture techniques (e.g., 3C, Hi-C) have enabled the determination of DNA structure and nuclear organization. As a consequence, studies on various organisms have observed that DNA replication timing is highly correlated with chromatin folding and global nuclear architecture [34–36]. In mammalian cells, chromatin conformation maps agree with replication timing profiles

more closely than any other chromatin property, independently establishing the existence of evolutionarily conserved units of temporally co-regulated replicons aligned with replication domains [37–41]. In budding yeast nuclei, early firing origins were found to be clustered [42]. A recent study in fission yeast identified a gradient of origin efficiency centered on the spindle pole body (SPB), suggesting a diffusion-based mechanism coordinating DNA replication [43].

A number of mathematical and computational models have attempted to elucidate the complex nature of DNA replication using different mathematical formulations, such as the KJMA framework [44, 45], anomalous reaction-diffusion and inhomogeneous replication kinetics [46, 47], probabilistic models of origin firing [48–50] and stochastic hybrid models [51, 52]. Using a model of DNA replication in HeLA cells that incorporates domino-like replication progression and random loop folding of chromatin, Löb et al. [53] were able to reproduce experimentally observed patterns in 3D. More recently, Arbona et al. [54] have modeled DNA replication as a spatio-temporal process, showing that the diffusion of firing factors alone is sufficient to account for characteristic replication kinetics captured by the probability of firing an origin per unit time and length of unreplicated DNA $I(t)$, a function that forms the basis of many mathematical models of DNA replication [44, 55, 56].

In this work, we set out to further elucidate the interplay between linear DNA replication, protein mobility dynamics and spatial chromatin structure. We present an integrated model for DNA replication that exploits three-dimensional genome structure and origin location data as derived by chromatin conformation experiments to simulate the spatio-temporal dynamics underlying origin firing. By explicitly modeling nuclear protein mobility, probabilistic origin firing and linear replication fork progression, we incorporate diffusion and binding dynamics to mechanistically describe the stochastic foundations of DNA replication. Analysis of a large number of *in silico* replication profiles enables the assessment of model parameter sensitivity and reveals spatial patterns that were independently validated *in vivo*. In summary, our model provides a framework to realistically simulate DNA replication across a complete genome, and to investigate the relationship between three-dimensional chromatin conformation and DNA replication timing.

2 Results

2.1 A stochastic, three-dimensional model of DNA replication

We present a spatio-temporal model of DNA replication that incorporates both protein and replisome movement within the nucleus to capture the stochastic nature of DNA replication timing. The model consists of two main modules: a **particle-centric** module that models the mobility of firing factors within the nucleus, and an **origin-centric** module that captures origin firing and linear progression of replisomes along the genome. Both modules are characterized by hybrid dynamics (e.g., continuous movement of replication forks, discrete binding/unbinding events) and stochasticity (e.g., firing factor diffusion, origin firing). Similar to the work by Arbona et al. [54], our model does not require experimentally derived origin efficiencies as input, but explicitly models origin firing as the interaction between firing factors and origin sites.

The spatio-temporal model simulates DNA replication at a whole-genome level and is tailored to the case of fission yeast, exploiting recent three-dimensional genome structures derived by chromosome conformation capture experiments [43, 57]. A graphical summary of the model is given in Fig. 1, and a full mathematical description is given in Supplementary Methods Section S1. A number of experimentally derived input parameters are required (Fig. 1A), such as the nuclear size and the replication fork speed. Provided that this information is available, the model can be extended to any eukaryotic organism. Model simulations yield *in silico* DNA replication profiles and allow the exploration of DNA replication dynamics for different hypotheses and/or parameter values. By repeatedly sampling from multiple independent simulations, both system-global and origin-specific statistics can be computed.

Nuclear architecture The processes and interactions described in both modules of our model take place within the nucleus (Fig. 1B - right). Following the work of [43, 57], the fission yeast nucleus is modeled as a three-dimensional spherical domain with impermeable boundaries excluding the nucleolus, the region containing ribosomal DNA repeats. The spindle-pole body (SPB), a nuclear sub-domain of special interest containing the centromeres [58, 59], is localized at the nuclear periphery, diametrically opposite of the nucleolus. Spatial origin coordinates were estimated by mapping the experimentally determined base-pair coordinates of Heichinger et al. [24] onto the three-dimensional whole-genome coordinates of Grand et al. [57] and Pichugina et al. [43].

Particle-centric module The particle-centric module of our model represents the behavior of the firing factors (hereafter referred to as particles) within the nucleus, based on previous work [60, 61]. Candidate proteins for this role are all molecular partners participating in origin firing via the formation of the pre-IC (e.g., Cdc45, Sld2 and Sld3). We collectively represent them as one class of particles, and assume that their count is fixed throughout S-phase. Each particle is characterized by three states: a continuous state representing the position of the particle in the nucleus, a discrete binary state

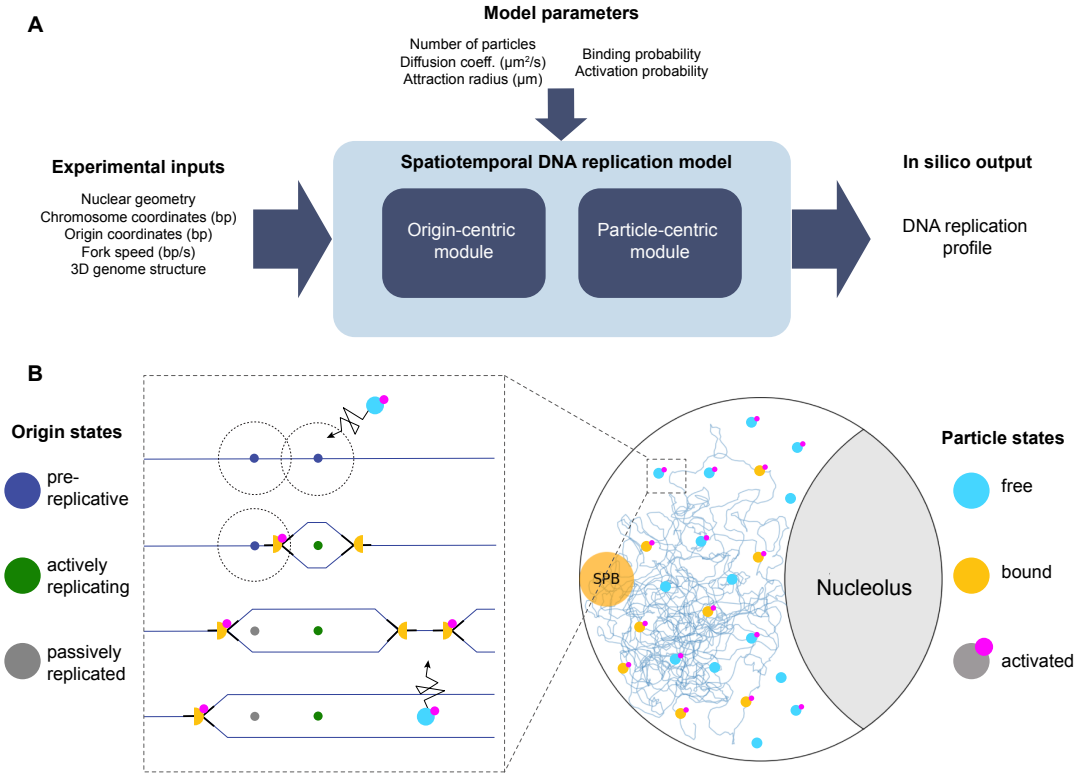

Figure 1: **(A) Overview of the DNA replication model.** Simulations of the DNA replication model with the required inputs (top: model parameters, left: experimentally-derived inputs) give rise to *in silico* DNA replication timing profiles. **(B) Schematic representation of the two modules.** Right: Firing factor particles, found at different discrete states, diffuse and bind within the nucleus. Left: An unbound and activated particle enters the attraction sphere (dotted circle) of a licensed replication origin, initiating firing and changing the discrete origin state to actively replicating. Two replication forks emanate and move along the linear DNA sequence in opposite directions, thereby replicating the genome. The particle splits into two monomers that travel along with the replication forks. Licensed origins that do not have the chance to fire before a fork passes through switch state to passively replicated. When forks moving in opposite directions collide, they merge and the newly-formed particle dimer is released to freely diffuse and potentially fire other licensed origins.

representing its binding status, and a discrete binary state representing its activation status (Fig. 1B - right and Fig. S1A). Particles diffuse freely in the nucleus if not bound to an origin. Particle diffusion is described by a stochastic differential equation and assumed to be isotropic, space-homogeneous and effective. The latter implicitly accounts for biophysical interactions, such as collisions with macromolecules or transient binding to DNA. Particles that attempt to diffuse out of the nucleus are reflected back using a boundary reflection scheme akin to [62]. A particle switches from inactivate to activate through phosphorylation by different kinases in the SPB (e.g., CDK, DDK), and between the free and bound states through its interaction with replication origins.

Origin-centric module The origin-centric module of our model is largely based on the stochastic hybrid model of Lygeros et al. [51]. Briefly, a replication origin can be in one of the following discrete states at any time: *Pre, RB, RL, RR, Post,* or *Pass* (Fig. S1B). Initially, all origins are assumed to be licensed and begin in the *Pre* (pre-replicative) state. Upon firing, replication forks start traveling in either direction, and the origin enters the *RB* state (replicating bidirectionally). Based on experimental evidence, the fork speed is assumed to be a constant of $v_{fork} = 50$ bases per second [24, 63]. When a fork collides with an incoming fork emanating from another origin, the initiating origin changes state from *RB* to *RL* or *RR* (replicating to the left / right) depending on whether the left or right fork is still active. Once both forks have collided and stopped replicating, the initiating origin switches to the *Post* (post-replicative) state and does not contribute to the replication process anymore. If a replication fork passes through an *Pre* origin that has not fired yet, it is blocked from future firing to prevent re-replication of DNA and enters the *Pass* (passively replicated) state. Replication is complete when all origins are in the *Pass* or *Post* state, which implies that all forks have either merged or reached the end of a chromosome.

Particle-origin interaction The crosstalk between the two modules is an essential aspect of our model and is orchestrated by particle-origin interactions (Fig. 1B - left). For origin firing to occur, an unbound and activated particle must diffuse into the attraction sphere of a *Pre*-state origin and bind to it (Fig. S1C). To capture the inherent stochasticity of this process, a parameter P_{bind} is introduced, representing the probability of a particle binding to an origin when it is within range. Upon firing, the particle splits into two monomers that travel along the genome with the replisomes. Upon fork convergence, the reassembled dimer is released to freely diffuse in the nucleus and potentially fire other origins (Fig. S1D). Particle state transitions are governed by stochastic dynamics, apart from the bound $\rightarrow$ free transition, which occurs when forks merge and is thus deterministic given the time of firing. Origin state transitions are governed by deterministic dynamics, apart from the *Pre* $\rightarrow$ *RB* transition, which is governed by the stochastic dynamics of particle binding. The tight interplay between the two modules is thus executed through these interlinked transitions, with particle dynamics affecting origin dynamics and *vice versa*.

Model variations To examine how nuclear architecture affects the replication process, we conducted multiple simulations under the following conditions:

1. **Random origin positioning:** The model is instantiated with genome structures that lie within the nuclear domain boundary, but were not fitted to proximity ligation data or other biological constraints [57, "confined" model]. Particles are initialized uniformly in the nucleus in the activated state, ready to bind to origins.
2. **Uniform particle initialization:** To examine whether origin localization within the nucleus affects the replication process, three-dimensional genome structures generated from genome conformation capture experiments are used as input [57, "interactions" model]. Particles are initialized as in model variation 1.
3. **SPB-mediated particle activation:** Experiments have shown that DNA closer to the SPB tends to replicate earlier [43]. The activation of firing factors in the SPB region has been hypothesized as a mechanistic explanation for these findings, as origins near the SPB would be the first exposed to firing factors [43]. In this model variation, the model is instantiated similarly to model variation 2, but with all particles in the inactivated state. To model the described behavior, particles are activated probabilistically upon diffusion into the SPB region, accounting for the stochastic nature of the underlying biochemical process. For each diffusion step within the SPB region, there is a probability of activation (P_{act}) if the particle has not yet been activated. SPB-mediated particle activation slowly introduces active particles to the nucleus and is equivalent to modeling an influx of particles from outside the nucleus through the SPB.

Implementation and simulations The numerical implementation and simulation of the continuous model was executed through a discrete approximation scheme [60] by gridding time and space according to a spatial resolution parameter h (Supplementary Methods Section S2). Previous work [62] has demonstrated that, under this scheme, as $h \to 0$, the approximate process converges in distribution to the original, continuous process. The joint model was implemented in a highly parallelized and modular fashion using C++ and MPI, with various optimizations to further increase simulation throughput. Visualizations of exemplary simulations can be found in the Supplementary Material; the source will be made publicly available upon publication.

2.2 Analysis of in silico replication profiles

To assess the validity of hypotheses and effects of parameter values in DNA replication timing, an initial set of Monte Carlo simulations was conducted for all model variations and a broad range of non-probabilistic parameter values. For model variation 1 (random origin positioning), 100 out of the 1000 genome structures from Grand et al. [57, "confined" model] were selected at random. For model variations 2 (uniform particle initialization) and 3 (SPB-mediated particle activation), three-dimensional genome

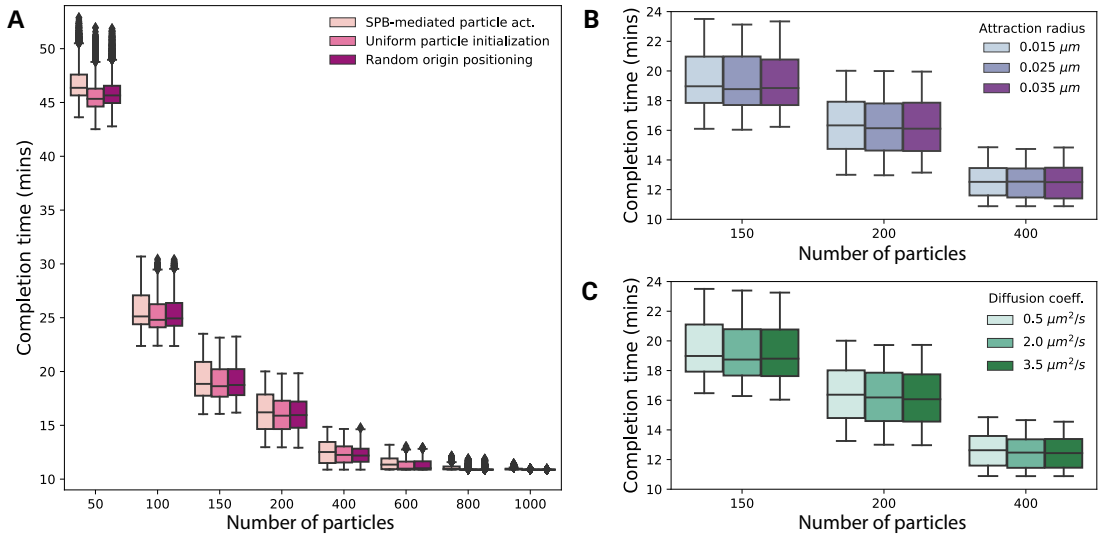

Figure 2: **Comparison of completion time distributions for different model variants and simulation parameters.** All sub-figures capture the complete set of simulations, as described in the main text, with varying values for all parameters. **(A)** Simulated completion times for the three model variants across a wide range of number of particles N. **(B)** Simulated completion times for three different attraction radii r_{attr}. **(C)** Simulation completion times for three different effective diffusion coefficients D.

structures generated from genome conformation capture experiments were used [43, 57]. Out of the available 1000 structures, a subset of 217 structures was selected to represent a population of fission yeast cells as detailed in Supplementary Methods Section S3. The parameter values examined were the following:

Number of particles (N)	$\{50, 100, 150, 200, 400, 600, 800, 1000\}$
Origin attraction radius (r_{attr})	$\{0.015\mu m, 0.025\mu m, 0.035\mu m\}$
Effective diffusion coefficient (D)	$\{0.5\mu m^2 s^{-1}, 2.0\mu m^2 s^{-1}, 3.5\mu m^2 s^{-1}\}$

Parameter values for the origin attraction radius r_{attr} were estimated based on crystal structures of the origin recognition complex [64] and the MCM2-7 double hexamer [65]. The particle binding and activation probabilities were set to $P_{bind} = P_{act} = 1$. To account for the stochastic nature of the replication process, five iterations were performed for each structure and parameter combination, resulting in a total number of 192,240 individual simulations. Simulations were performed on an IBM Power System S822LC, with individual execution times largely dependent on the parameter choices. For each simulation, origin firing times and total time until completion were recorded.

DNA replication completion time

Because the time until completion of DNA replication time has been experimentally established in fission yeast [66], it is an important indicator of the model's ability to reflect biological reality. The results of the initial simulation runs show that the completion time is largely dominated by the number of particles present in the nucleus (Fig. 2). With 50 particles, most replication cycles complete in 45 to 50 minutes, a number which decreases exponentially as N increases. Notably, at high N, the completion time converges to the minimum theoretical completion time of 652.92 seconds, equivalent to the time needed to replicate the maximum inter-origin distance from Heichinger et al. [24]. From all tested values of number of particles, simulations with $N = 150$ achieved the reported completion time of 20 minutes in fission yeast [66].

The effect of the diffusion coefficient and attraction radius on the distribution of completion times was negligible when N was held constant (Fig. 2), despite the exploration of a broad range of plausible values for both parameters. Similarly, the model variant did not have a significant impact on the completion time. Replication utilizing SPB-mediated activation of particles tended to take slightly longer than the other two variants, as apparent for low numbers of N. This result is expected, because particles must diffuse to the SPB to be activated before binding to origins. However, the impact on completion time is minimal, indicating empirically that the timescale of particle diffusion throughout the nucleus is much shorter than that of replication forks moving along DNA strands.

Spatial organization of origin firing

To examine the spatial organization of replication timing in the nucleus, relative radial kernel density estimates (KDEs) were calculated for experimentally derived origin efficiencies [24] and for the average simulated origin efficiencies from the three model variants (Supplementary Methods Section S4.1). Two types of KDE plots were computed. The KDEs of average origin efficiencies and activation times across all simulations and structures is shown in Fig. 3. Due to variety in structure data, we also found it illuminating to compute a per-structure average KDE from the same data (included in Supplementary Fig. S3) to provide the most detailed view of the relationship between origin location and firing. In the efficiency KDE plots in Fig. 3A, the SPB-mediated particle activation model variant shows a pattern of efficiencies most similar to the experimental data: efficient origins tend to co-locate with the SPB, whereas inefficient origins tend to be located near the periphery, far from the SPB. KDE plots of origin firing times (Fig. 3B) also show similarities between SPB-mediated particle activation and experimental data, with early-firing origins located close to the SPB and late-firing origins close to the periphery and nucleolus. KDE plots of average efficiencies and firing times for individual structures rather than an average over all simulations, shown in Fig. S3, reveal efficient yet late-firing origins near the nucleolus in addition to those near the SPB, suggesting a wave-like origin firing behavior. As expected, the random origin positioning variant

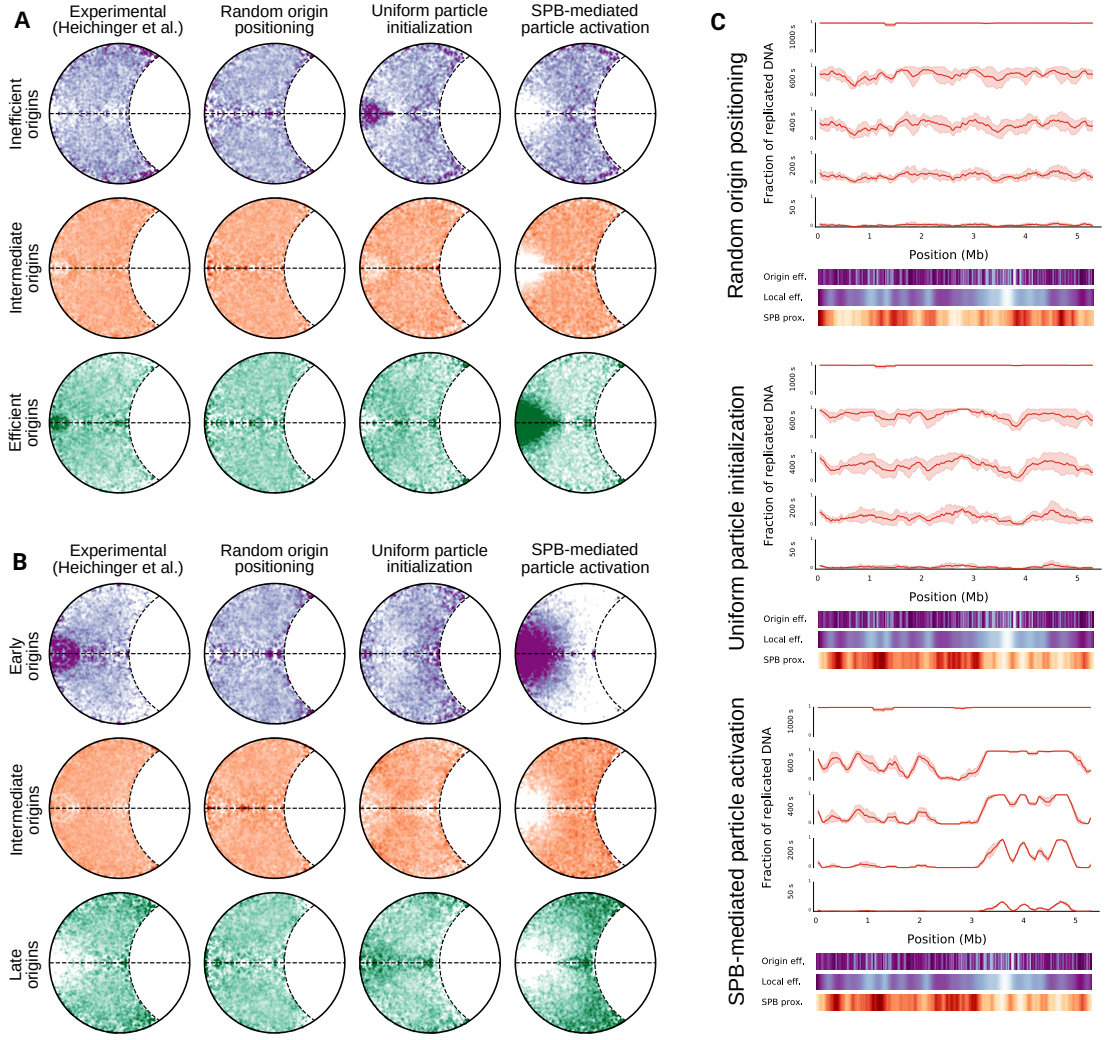

Figure 3: **Spatial organization of average origin efficiency and firing times. (A)** Relative radial kernel density estimates of inefficient (lower quartile efficiencies, top row), intermediate (Q1 < efficiency < Q3, middle row), and efficient (upper quartile efficiencies, bottom row) origins. **(B)** Relative radial kernel density estimates of early-firing (firing time < Q1, top row), intermediate (Q1 < firing time < Q3, middle row), and late-firing (firing time > Q3, bottom row) origins. **(C)** Evolution of replicated DNA over time for Chromosome 1 and all three model variants (top: random origin positioning, middle: uniform particle initialization, bottom: SPB-mediated particle activation). The red line corresponds to mean fraction of replicated DNA across all five single-structure simulations and the shaded area to the corresponding standard deviation. Color bars show experimental origin efficiency, local origin efficiency (Supplementary Methods Section S4.2), and SPB proximity at a given coordinate (lighter color ... higher efficiency / closer to SPB).

shows a uniform, random distribution of efficient and inefficient origins, as well as early and late-firing origins, with no discernible pattern. Surprisingly, uniform particle initialization using experimentally derived genome structures results in inefficient origins in the SPB region. This is likely the result of a higher density of origins near the SPB in the underlying structure.

Next, to elucidate the dynamic evolution of DNA replication progresses with respect to nuclear organization, we computed the fraction of replicated DNA over time for single-structure simulations and all model variants (Fig. 3C). In contrast to the random origin and uniform particle initialization variants, where DNA replication initiation appears random and shows high variability across simulations, SPB-mediated particle activation leads to consistent early replication of the SPB region, as shown for Chromosome 1 in Fig. 3C. These early peaks of replicated DNA coincide with the two previously reported most efficient regions of the chromosome [24], and additionally correlate strongly with SPB proximity. The timing of replication for other regions of the chromosome depends on the underlying 3D structure, as regions closer to the SPB tend to replicate first.

2.3 In vivo exploration of spatial organization

Since the SPB-mediated particle activation model variant best fits the experimental data, we set out to independently validate our conclusions *in vivo*. Based on our *in silico* predictions, replication initiates with a higher probability from SPB-proximal origins, which are more accessible to freely diffusing activated particles. To monitor early replication events *in vivo*, we performed immunofluorescence against the thymidine analog BrdU, which marks nascent DNA, in fission yeast cells arrested in early S phase using hydroxyurea (HU). The strain bares also the centromeric protein Mis6 tagged with GFP. We observed a strict BrdU incorporation pattern surrounding centromeres in early S phase (Fig. 4A), confirming the model prediction. Upon centromere clustering disruption (Csi1Δ), the BrdU/Hoechst ratio increases significantly (p-value $= 1.5 \cdot 10^{-4}$), indicating a more dispersed incorporation pattern (Fig. 4A, B) and suggesting that indeed the SPB acts as a positive pole for replication initiation.

To investigate the correlation between distance from SPB and origin efficiency more thoroughly, we tagged one efficient and one inefficient origin [24] in each chromosome using the lacO-lacI system in Mis6-mCherry background fission yeast strains (Fig. 4C). The three-dimensional Euclidean distance between the SPB and the origin was measured microscopically for each individual tagged origin and plotted for each chromosome (Fig. 4D). In agreement with the simulated data for the SPB-mediated particle activation model, the efficient origins (orange) are positioned more proximally to the centromeres-SPB structure compared to the inefficient ones (blue) (p-values $= 5.6 \cdot 10^{-6}, 5.3 \cdot 10^{-7}$, and $6.3 \cdot 10^{-8}$ for origin pairs in Chromosomes 1, 2, and 3, respectively). The efficiency of each origin was independently verified by real-time quantitative PCR (qPCR, Fig. 4E). All p-values were computed using a standard Mann-Whitney statistical test.

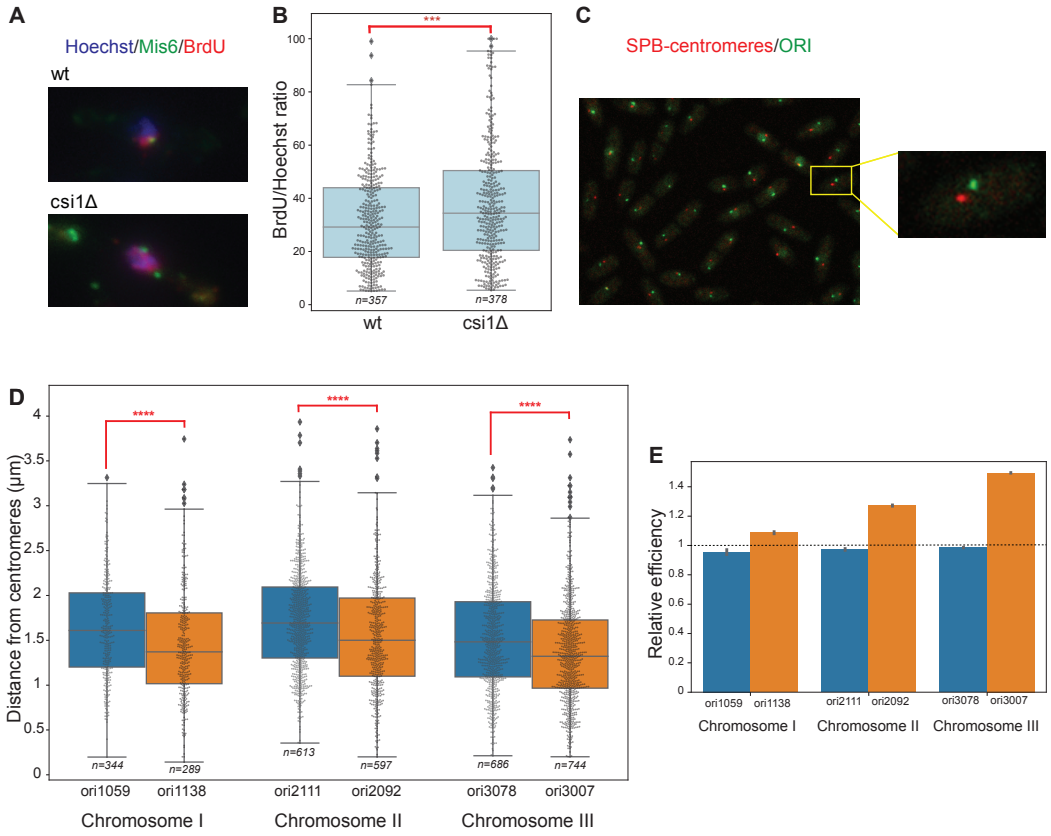

Figure 4: ***In vivo* exploration of spatial organization.** **(A)** Immunofluorescence against BrdU in Mis6-GFP wild type and Mis6-GFP Csi1Δ fission yeast cells arrested in early S using HU. Mis6 marks the centromeres (green), BrdU the stains for nascent DNA (red) and Hoechst stains the whole nucleus (blue). **(B)** BrdU/Hoechst area ratio (in percent), plotted for wild type and Csi1Δ cells. **(C)** Tagging of specific origins using the lacO-lacI system in a Mis6-mcherry background strain. A representative image is shown. **(D)** For each chromosome, the 3D distance to the centromeres/SPB structure for one efficient (orange) and one inefficient (blue) origin was measured microscopically. **(E)** The efficiencies of the respective origins were validated by real-time qPCR.

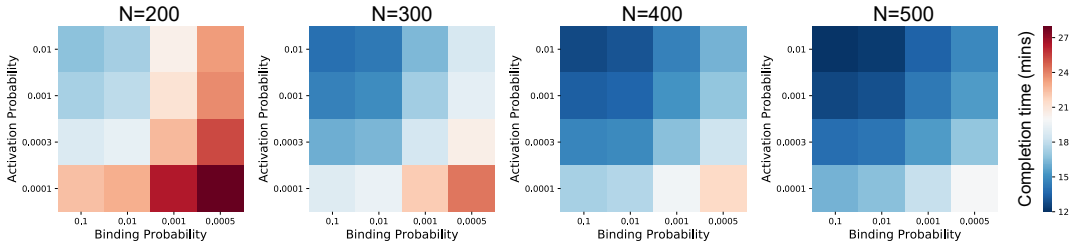

Figure 5: **Sensitivity analysis of model probabilities.** Mean completion time (in minutes) for various combinations of model parameters and number of particles N, shown on a diverging color scale centered on the desired completion time of 20 minutes.

2.4 Exploration of model probabilities

The number of particles N has been shown to be an influential parameter, and both our *in vivo* and *in silico* analyses indicated that SPB-mediated particle activation produces the most realistic results out of all model variants. Therefore, a second set of simulations was conducted to explore N in more detail as well as to observe the effect of different values of the binding and activation probabilities. Structures and constants were left unchanged from the previous set of simulations, and the origin attraction radius and the effective diffusion coefficient were set to $r_{attr} = 0.025\mu m$ and $D = 0.5\mu m^2 s^{-1}$, respectively. Only model variation 3 (SPB-mediated particle activation) was considered, and all combinations of the following parameter values were examined:

Number of particles (N)	$\{150, 200, 250, 300, 350, 400, 450, 500\}$
Particle binding probability (P_{bind})	$\{0.1, 0.01, 0.001, 0.0005\}$
Particle activation probability (P_{act})	$\{0.01, 0.001, 0.0003, 0.0001\}$

Sensitivity analysis

We first examined the effect of different model probabilities on the DNA replication completion times for various values of the number of particles N, shown as heatmaps in Fig. 5 (for brevity, heatmaps are not shown for all values of N). Completion times ranged from 12 minutes to about half an hour. For the parameter sets shown, there are many combinations that achieve the desired completion time of 20 minutes, generally showing a trade-off between binding probability and activation probability to maintain the same completion time. As expected, decreasing P_{bind} or P_{act} increases the overall completion time, so the completion time is highly tunable for any value of N.

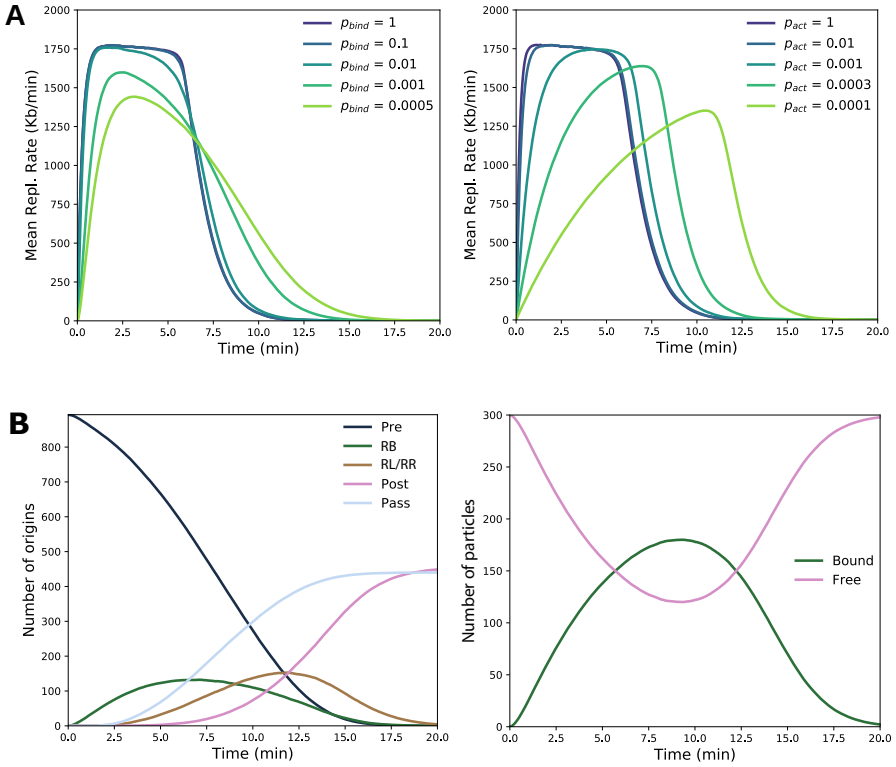

Figure 6: **Summary of replication kinetics for different parameter values.** In all simulations, $N = 300$, $r_{attr} = 0.025\mu m$, and $D = 0.5\mu m^2 s^{-1}$. **(A)** Left: Effect of P_{bind} on mean replication rate ($P_{act} = 0.01$). Right: Effect of P_{act} on mean replication rate ($P_{bind} = 0.1$). **(B)** Left: Average number of origins in each model state over the course of replication for a single parameter set ($P_{bind} = 0.001$, $P_{act} = 0.0001$). Right: The corresponding average number of free and bound particles.

DNA replication kinetics

We next assessed how model probabilities affect the kinetics of DNA replication in terms of mean replication rate (Supplementary Methods Section S4.3). As shown in Fig. 6A, binding probability primarily affects mid to late S phase. High values of P_{bind} lead to almost immediate binding of nearly all particles to origins within the first couple of minutes and result in a relatively constant and high replication rate, that abruptly decreases shortly before the end of replication. Conversely, low values of P_{bind} delay the particles from binding to origins and increase the pool of free particles. This slows down the replication kinetics, significantly reduces the maximum replication rate reached and results in a more gradual rather than sharp decline. Similarly to P_{bind}, high values of P_{act} lead to a sharply increasing and high replication rate. However, decreasing P_{act} has a more prominent effect in the beginning of S phase. Low P_{act} will both delay and decrease the maximum replication rate: a lower P_{act} slows down the particles' activation

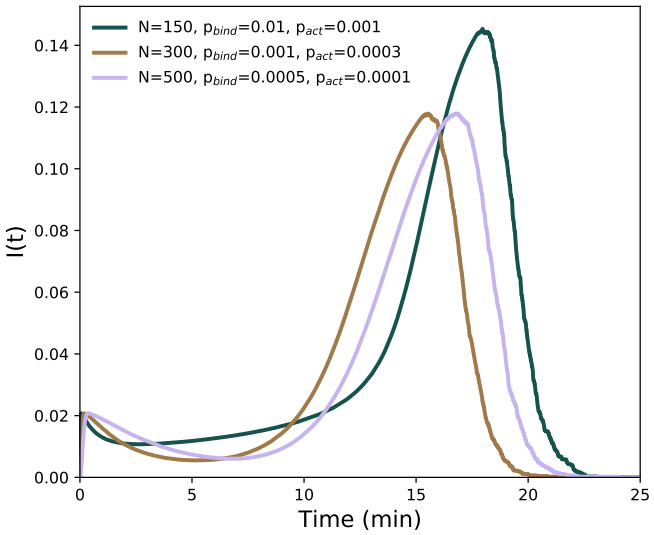

Figure 7: **Probability of initiating an origin per unit time and per length of unreplicated DNA** $I(t)$**.** Mean $I(t)$ for a variety of parameter sets, obtained from 500 simulations for each curve, resembling the characteristic bell shape observed in eukaryotes [67]. In all simulations, $r_{attr} = 0.025\mu m$ and $D = 0.5\mu m^2 s^{-1}$.

rate that subsequently need more time to bind to and fire the origins. As indicated in the plots, a P_{act} of 0.0003 will lead to a peak around 10 minutes, which would approximately correspond to mid S phase.

A detailed view of DNA replication kinetics combining probabilistic activation and binding ($P_{act} = 0.0001$, $P_{bind} = 0.001$) is shown in Fig. 6B. Tracking the number of origins in each model state provides insight into replication kinetics. The number of origins in the Pre state steadily decreases from 893 to 0 throughout replication. The number of origins in the RB state peaks before the number in RL or RR, as expected because forks do not begin to collide until a few minutes after origins begin firing. Most passive replication occurs during mid S phase, when the overall replication rate is at a maximum, whereas the transition from RL or RR to $Post$ occurs primarily during mid to late S phase, when the replication rate is decreasing. The number of bound particles, which is proportional to the replication rate, exhibits a bell-shaped profile with a gradual rise and fall and a peak in mid S phase, agreeing with experimental evidence [63].

Probability of initiating an origin per unit time and length of unreplicated DNA

The "probability of initiating an origin per unit time and per length of unreplicated DNA" introduced by Herrick et al. [67] forms the basis of many mathematical models of DNA replication [44, 55, 56]. This function, denoted $I(t)$, where t is the time since the start of S phase, resembles a universal bell-curve shape in eukaryotes, peaking in mid- to

late- S phase. Goldar et al. developed a mathematical model postulating the presence of a limiting factor that binds to unreplicated locations of the DNA initiating replication and is released upon fork convergence [44]. Arbona et al. [54] demonstrated that a bell-shaped $I(t)$ arises from a DNA replication model incorporating a fixed number of firing factors that bind to origins, move along the DNA, and release upon fork collision.

Because our stochastic hybrid model is similar to the model used by Arbona et al., we were able to reproduce the characteristics of their simulated $I(t)$ profile for a variety of parameter sets. Briefly, $I(t)$ is a fraction with the probability of initiating an origin per unit time in the numerator (proportional to number of free particles $\times$ number of *Pre*-state origins) and the length of unreplicated DNA in the denominator. Since in our model we actively track both particles and origins at different states, the *in silico* $I(t)$ profile can be computed in a straightforward way (Supplementary Methods Section S4.4). $I(t)$ profiles of simulations with varying parameters are shown in Fig. 7, capturing the characteristic peak behavior and, as expected, bearing a high resemblance to the results of Arbona et al. [54]. From early until mid S phase, $I(t)$ decreases slightly due to both the number of free particles and pre-replicative origins decreasing. After mid S phase, fork collisions lead to an increasing number of free particles. Together with the decreasing amount of unreplicated DNA in the denominator, they lead to a sharp increase and peak of $I(t)$. At the end of replication, the number of pre-replicative origins tends to zero, causing a rapid decline of $I(t)$.

This qualitative behavior of $I(t)$ is not sensitive to parameter changes within the parameter sets we explored, though Arbona et al. showed that extreme parameter values distort the curve [54]. We thereby confirm their conclusion that the bell-shaped $I(t)$ curve arises from a limited number of particles in conjunction with recycling of firing factors upon fork collision.

2.5 Origin firing concurrence

Recent experimental evidence has reported the presence of clusters of fired origins in late S phase, organized in nuclear replication foci [63]. To assess this effect *is silico*, we computed the tendency of all pairs of origins across the genome to fire concurrently (Supplementary Methods Section S4.5). The results across the whole genome for large (A) and small (B) values of the binding probability are visualized using heatmaps (Fig. 8), where pairs of origins that fire together in the same replication cycle are shown in blue, and pairs with a competitive relationship are shown in red. As can be easily assessed, most pairs of origins are uncorrelated with each other, but patterns emerge near the diagonal of the matrix, representing origins that are close to each other on the linear DNA sequence.

Since particles are activated in the SPB, we expect that some degree of firing concurrence will result from the three-dimensional structure of the genome. Nearby origins should be found together in particle-rich or particle-poor regions, due to genome structure and

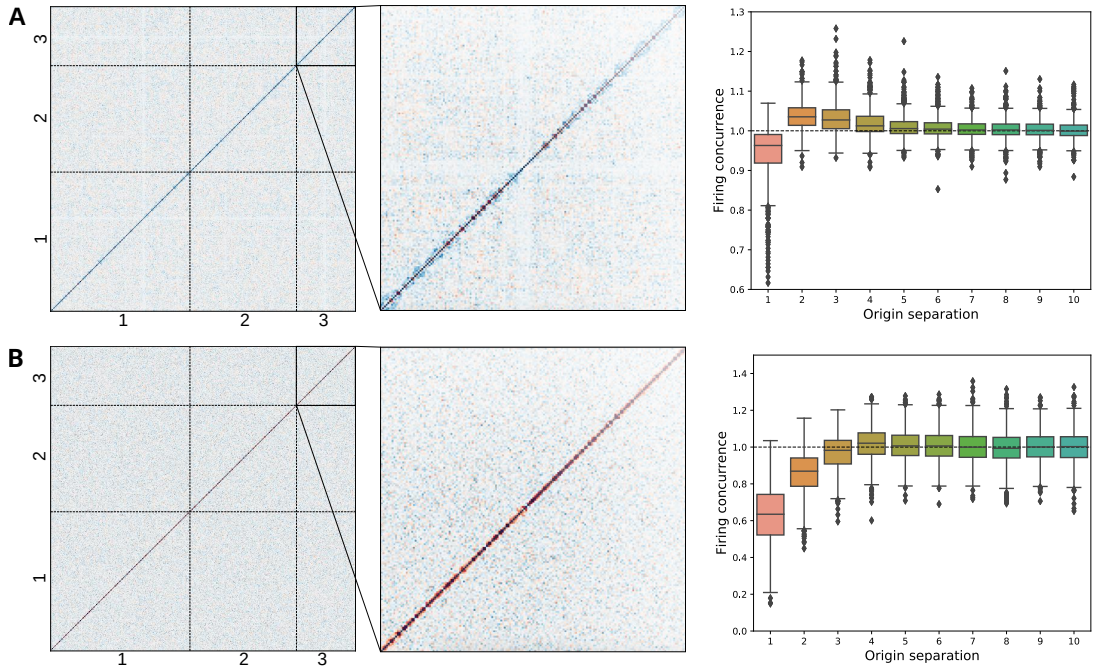

Figure 8: **Neighborhood effects on origin firing.** In all parameter sets, $N = 150$, $D = 0.5\mu m^2 s^{-1}$, $r_{attr} = 0.025\mu m$, and $P_{act} = 0.01$. **(A)** Concurrence matrix with inset showing Chromosome 3 (left) and distributions of firing concurrence for neighboring origins (right), demonstrating local concurrence when $P_{bind} = 0.1$. **(B)** Concurrence matrix with inset (left) and distributions of firing concurrence (right), demonstrating strong local competition when $P_{bind} = 0.0005$.

the nature of SPB-mediated particle activation. When P_{bind} is relatively large (Fig. 8A), the blue halo around the diagonal in the concurrence matrix indicates that origins in the same region are likely to fire together, since particles are unlikely to diffuse away before binding to an origin thus negating structural effects. This is also clear in the boxplots of firing concurrence, which show that origin firing is correlated within a neighborhood of about five origins. In contrast to the general firing concurrence within a neighborhood, adjacent origins exhibit a competitive relationship, obvious from the red super- and sub-diagonals of the concurrence matrix and the boxplot of the nearest neighboring origin. The reason for this effect is twofold: passive replication is likely to occur when one origin fires, thereby prohibiting its neighbors from firing; and origin firing decreases the concentration of particles in the region because a particle binds to the replicating origin and cannot fire other, nearby origins.

Conversely, when P_{bind} decreases (Fig. 8B), the concurrence patterns point to strong competition in firing within an origin's neighborhood, indicated by both strong red around the diagonal of the concurrence matrix and negative firing concurrence values up to the three nearest neighboring origins. This effect is expected: for low binding

probabilities, particles are able to diffuse away and explore the nucleus before binding to an adjacent origin, giving the chance to forks emanating from the fired origin to passively replicate the neighborhood. To further investigate this effect, we computed the cumulative frequency of inter-origin distances (IODs), as previously demonstrated by Kaykov and Nurse [63] (Supplementary Methods Section S4.6). The experimentally observed clustering effects [63] cannot be explained by structure alone. Indeed, the opposite effect is observed *in silico* as shown in Fig. S4: origins tend to fire more sparsely than they would if randomly distributed, due to competition between neighbors caused by passive replication.

3 Discussion

A spatio-temporal model of DNA replication

In this work a particle-based, spatio-temporal model of DNA replication is presented. Similar to Arbona et al. [54], our model explicitly simulates the diffusion of firing factor particles within the nucleus, their interaction with replication origins that leads to origin firing, and the movement of replication forks along the genome. It can thus capture the complex stochastic hybrid dynamics that govern the DNA replication process, with discrete dynamics associated with origin and particle states and continuous dynamics associated with particle diffusion and replication fork movement. Particle dynamics affect origin dynamics and *vice versa*, captured by interlinked transitions that represent stochastic origin firing or deterministic fork collisions.

Our model is tailored to the case of fission yeast; however, it is versatile and can be adapted to different nuclear geometries and/or experimental inputs, thus easily extended to more complex eukaryotes. It incorporates a number of parameters, such as the number or effective diffusion coefficient of particles, and two probabilities that account for the stochastic nature of particle binding and activation. Three variations of the model were implemented, corresponding to different hypotheses concerning origin positioning and particle initialization within the nucleus: origins are positioned either randomly or at experimentally-derived three-dimensional positions [43, 57]; particles are either initialized uniformly and already in the activated state, or must diffuse into the SPB region to get activated. These variations allow us to investigate spatial patterns of DNA replication and mechanisms concerning origin firing.

Model parameters affecting DNA replication completion

The resulting *in silico* replication profiles allowed us to gather statistics on DNA replication timing, such as time until completion of DNA replication. This analysis indicated that the number of particles N strongly affects the time needed for a full DNA replication, with at least 150 particles necessary to complete replication within the experimentally established 20 minutes limit [66]. The number of particles appears to be rate-limiting, since, when N increases and reaches the number of origins, the completion time converges to the minimum time needed to replicate the largest inter-origin distance, indicating immediate firing of all origins. This agrees with extensive experimental evidence from the literature, reporting that replication factors that participate in origin firing exist in limiting quantities [28, 68–71], and with our prior *in silico* analysis [51], where the presence of a limiting factor that is continuously redistributed in origins during replication is a plausible explanation of the so-called random gap problem [72].

On the contrary, parameters such as origin attraction radius and effective diffusion coefficient are insignificant to completion time. Even with a low effective diffusion coefficient of $D = 0.5\mu m^2 s^{-1}$, a particle would traverse the $2.66\mu m$ nuclear diameter in about seven seconds, a much smaller timescale than that of the entire replication process, giving it enough time to explore the nucleus for origin binding sites. Further, different model variations indicated negligible effects on completion times, with minimally longer completion times observed when the SPB-mediation activation variant was simulated, particularly for small N. This is likely also attributed to the faster timescale of diffusion: even if particles need to travel to the SPB to get activated, the delay introduced is minimal.

Nuclear organization and DNA replication

Recent evidence pointed to a diffusion-based pattern of origin firing, manifested as a gradient of origin firing time and efficiency centered at the SPB [43]. Our model is able to capture this spatial pattern for high binding probabilities when an SPB-mediated particle activation is assumed. Indeed, *in silico* profiles corresponding to this variation indicate that SPB-proximal origins fire early and efficiently, and, as the process continues, the firing factor particles are released and redistributed to the remaining origins. By the end of replication, the increased availability of unbound particles leads to the late yet efficient firing of nucleolus-proximal origins. The SPB-dependent firing pattern observed *in silico* was independently assessed *in vivo*. Immunofluorescence and real-time qPCR experiments in fission yeast cells validated that, indeed, DNA replication initiates from SPB-proximal origins, and that this pattern is lost once the nuclear architecture is distorted. These findings suggest that firing factor particles must diffuse to the SPB to get activated before they can bind to origins, possibly through their phosphorylation by different kinases such as CDK or DDK, or, alternatively, that they are introduced in the nucleus already in the activated state through SPB-specific nuclear pores.

The probabilistic nature of particle-origin interactions

As expected, incorporating probabilistic particle activation and binding extends the time to completion of DNA replication, with P_{act} mostly delaying early S phase and P_{bind} mostly delaying mid to late S phase. Increasing the number of particles N counteracts this effect, and multiple combinations of P_{act}, P_{bind} and N result in realistic completion times of 20 minutes, reflecting the model's adaptability. However, covering a broad range of parameter values, the number of particles N remained rate-limiting in all cases. In addition to the correct completion time, exploration of DNA replication kinetics for different combinations of the model parameters (N, P_{act}, P_{bind}) indicated that at least 300 particles would be a more realistic number to reproduce the experimentally observed bell-curve replication rate [63]. This is consistent with the observation of up to 400 replicons during replication of the *S. pombe* genome through DNA combing experiments, which suggests that at least 400 particles are necessary [63].

Published models of DNA replication have studied both *in vivo* and *in silico* the probability of initiating an origin per unit time and length of unreplicated DNA ($I(t)$), and have reported a profile of $I(t)$ common to many eukaryotes with a peak near the end of S phase [56]. In agreement with Arbona et al. [54], our simulation results support such a model, as the characteristic $I(t)$ profile is reproduced: $I(t)$ increases during S phase, at first slowly and progressively more rapidly, before collapsing near the end. In contrast to existing work that postulated an increasing availability of the limiting factor coupled with a binding probability correlated to active fork density to explain the results, in our case no such assumption is necessary, since the profile can be reproduced assuming only that the firing factor exists in limiting quantities.

Neighborhood effects

As discussed, our model can reproduce the global spatial pattern of origin firing for high probabilities. Additionally, a genome-wide analysis of origin firing concurrence indicated that, for larger values of P_{bind}, linearly-proximal origins are likely to fire together, since particles tend to bind to neighboring origins and fire them before they diffuse away. However, when P_{bind} is small, particles are able to explore the nucleus before re-binding to an origin, and as a result the spatial patterns are lost. Neighboring origins appear to compete in firing, since replication forks emanating from the origin that fired passively replicate and thus prohibit the neighboring origins from firing. For the same reason, the presence of replication foci observed in experiment [63] cannot be reproduced.

Therefore, the constant, uniform binding probability used in this model is too simple to capture more fine, local patterns of DNA replication, and our results suggest that more complicated mechanisms are probably in place. Origins may start with non-uniform binding probabilities corresponding to structural characteristics, such as AT content or intergenic size, which have long been reported to correlate with efficiency [20–24]. Binding probabilities may change over time depending on the progress of replication or nearby firing events. Alternatively, simulating more than one particle species that diffuse within the nucleus and progressively bind to and fire origins may be a more realistic scenario that implicitly reduces each origin's firing efficiency depending on it's location. Last, important limitations are introduced by the experimental structures themselves: although invaluable for the simulation of such models, they still lack the fine resolution needed to reproduce local clusters of replication domains. Future extensions of the model will allow us to investigate these mechanisms.

Acknowledgements

We thank Dr. Justin M. O'Sullivan and Dr. Tatyana Pichugina (Liggins Institute, University of Auckland, New Zealand) for their support in chromosome conformation capture data analysis and modeling. The work by J.L. was supported by SystemsX.ch under the project SignalX.

References

[1] Stephen P. Bell and Anindya Dutta. "DNA Replication in Eukaryotic Cells". In: *Annual Review of Biochemistry* 71.1 (June 2002), pp. 333–374. ISSN: 0066-4154, 1545-4509. DOI: 10.1146/annurev.biochem.71.110601.135425.

[2] Hideo Nishitani et al. "The Cdt1 protein is required to license DNA for replication in fission yeast". In: *Nature* 404.6778 (Apr. 2000), pp. 625–628. ISSN: 0028-0836, 1476-4687. DOI: 10.1038/35007110.

[3] Dirk Remus et al. "Concerted Loading of Mcm2–7 Double Hexamers around DNA during DNA Replication Origin Licensing". In: *Cell* 139.4 (Nov. 2009), pp. 719–730. ISSN: 00928674. DOI: 10.1016/j.cell.2009.10.015.

[4] Ioanna-Eleni Symeonidou et al. "Multi-step Loading of Human Minichromosome Maintenance Proteins in Live Human Cells". In: *Journal of Biological Chemistry* 288.50 (Dec. 13, 2013), pp. 35852–35867. ISSN: 0021-9258, 1083-351X. DOI: 10.1074/jbc.M113.474825.

[5] Nishitani Nishitani. "DNA replication licensing". In: *Frontiers in Bioscience* 9.1 (2004), p. 2115. ISSN: 10939946, 10934715. DOI: 10.2741/1315.

[6] Ioanna-Eleni Symeonidou, Stavros Taraviras, and Zoi Lygerou. "Control over DNA replication in time and space". In: *FEBS Letters* 586.18 (Aug. 31, 2012), pp. 2803–2812. ISSN: 00145793. DOI: 10.1016/j.febslet.2012.07.042.

[7] Matthew D. Ramer et al. "Dbf4 and Cdc7 Proteins Promote DNA Replication through Interactions with Distinct Mcm2–7 Protein Subunits". In: *Journal of Biological Chemistry* 288.21 (May 24, 2013), pp. 14926–14935. ISSN: 0021-9258, 1083-351X. DOI: 10.1074/jbc.M112.392910.

[8] L. Zou. "Formation of a Preinitiation Complex by S-phase Cyclin CDK-Dependent Loading of Cdc45p onto Chromatin". In: *Science* 280.5363 (Apr. 24, 1998), pp. 593–596. ISSN: 00368075, 10959203. DOI: 10.1126/science.280.5363.593.

[9] Y. Kamimura. "Sld3, which interacts with Cdc45 (Sld4), functions for chromosomal DNA replication in Saccharomyces cerevisiae". In: *The EMBO Journal* 20.8 (Apr. 17, 2001), pp. 2097–2107. ISSN: 14602075. DOI: 10.1093/emboj/20.8.2097.

[10] Seiji Tanaka et al. "CDK-dependent phosphorylation of Sld2 and Sld3 initiates DNA replication in budding yeast". In: *Nature* 445.7125 (Jan. 2007), pp. 328–332. ISSN: 0028-0836, 1476-4687. DOI: 10.1038/nature05465.

[11] S. Tanaka et al. "Efficient Initiation of DNA Replication in Eukaryotes Requires Dpb11/TopBP1-GINS Interaction". In: *Molecular and Cellular Biology* 33.13 (July 1, 2013), pp. 2614–2622. ISSN: 0270-7306. DOI: 10.1128/MCB.00431-13.

[12] J.-K. Lee, Y.-S. Seo, and J. Hurwitz. "The Cdc23 (Mcm10) protein is required for the phosphorylation of minichromosome maintenance complex by the Dfp1-Hsk1 kinase". In: *Proceedings of the National Academy of Sciences* 100.5 (Mar. 4, 2003), pp. 2334–2339. ISSN: 0027-8424, 1091-6490. DOI: 10.1073/pnas.0237384100.

[13] Max E. Douglas et al. "The mechanism of eukaryotic CMG helicase activation". In: *Nature* 555.7695 (Feb. 28, 2018), pp. 265–268. ISSN: 0028-0836, 1476-4687. DOI: 10.1038/nature25787.

[14] Dirk Remus and John FX Diffley. "Eukaryotic DNA replication control: Lock and load, then fire". In: *Current Opinion in Cell Biology* 21.6 (Dec. 2009), pp. 771–777. ISSN: 09550674. DOI: 10.1016/j.ceb.2009.08.002.

[15] Juan Méndez and Bruce Stillman. "Perpetuating the double helix: molecular machines at eukaryotic DNA replication origins: Review articles". In: *BioEssays* 25.12 (Dec. 2003), pp. 1158–1167. ISSN: 02659247. DOI: 10.1002/bies.10370.

[16] Hiroyuki Araki. "Elucidating the DDK-dependent step in replication initiation". In: *The EMBO Journal* 35.9 (May 2, 2016), pp. 907–908. ISSN: 0261-4189, 1460-2075, 0261-4189, 1460-2075. DOI: 10.15252/embj.201694227.

[17] Nicholas Rhind, Scott Cheng-Hsin Yang, and John Bechhoefer. "Reconciling stochastic origin firing with defined replication timing". In: *Chromosome Research* 18.1 (Jan. 2010), pp. 35–43. ISSN: 0967-3849, 1573-6849. DOI: 10.1007/s10577-009-9093-3.

[18] Nicholas Rhind. "DNA replication timing: random thoughts about origin firing". In: *Nature Cell Biology* 8.12 (Dec. 2006), pp. 1313–1316. ISSN: 1465-7392, 1476-4679. DOI: 10.1038/ncb1206-1313.

[19] Ioannis Legouras et al. "DNA replication in the fission yeast: robustness in the face of uncertainty". In: *Yeast* 23.13 (Oct. 15, 2006), pp. 951–962. ISSN: 0749503X, 10970061. DOI: 10.1002/yea.1416.

[20] J. Dai, R.-Y. Chuang, and T. J. Kelly. "DNA replication origins in the Schizosaccharomyces pombe genome". In: *Proceedings of the National Academy of Sciences* 102.2 (Jan. 11, 2005), pp. 337–342. ISSN: 0027-8424, 1091-6490. DOI: 10.1073/pnas.0408811102.

[21] Jia Xu et al. "Genome-wide identification and characterization of replication origins by deep sequencing". In: *Genome Biology* 13.4 (2012), R27. ISSN: 1465-6906. DOI: 10.1186/gb-2012-13-4-r27.

[22] Mónica Segurado, Alberto de Luis, and Francisco Antequera. "Genome-wide distribution of DNA replication origins at A+T-rich islands in *Schizosaccharomyces pombe*". In: *EMBO reports* 4.11 (Nov. 2003), pp. 1048–1053. ISSN: 1469221X. DOI: 10.1038/sj.embor.7400008.

[23] Makoto Hayashi et al. "Genome-wide localization of pre-RC sites and identification of replication origins in fission yeast". In: *The EMBO Journal* 26.5 (Mar. 7, 2007), pp. 1327–1339. ISSN: 0261-4189, 1460-2075. DOI: 10.1038/sj.emboj.7601585.

[24] Christian Heichinger et al. "Genome-wide characterization of fission yeast DNA replication origins". In: *The EMBO Journal* 25.21 (Nov. 1, 2006), pp. 5171–5179. ISSN: 0261-4189, 1460-2075. DOI: 10.1038/sj.emboj.7601390.

[25] C. Cayrou et al. "Genome-scale analysis of metazoan replication origins reveals their organization in specific but flexible sites defined by conserved features". In: *Genome Research* 21.9 (Sept. 1, 2011), pp. 1438–1449. ISSN: 1088-9051. DOI: 10.1101/gr.121830.111.

[26] Olivier Hyrien. "Peaks cloaked in the mist: The landscape of mammalian replication origins". In: *The Journal of Cell Biology* 208.2 (Jan. 19, 2015), pp. 147–160. ISSN: 0021-9525, 1540-8140. DOI: 10.1083/jcb.201407004.

[27] Prasanta K. Patel et al. "DNA Replication Origins Fire Stochastically in Fission Yeast". In: *Molecular Biology of the Cell* 17.1 (Jan. 2006), pp. 308–316. ISSN: 1059-1524, 1939-4586. DOI: 10.1091/mbc.e05-07-0657.

[28] O. M. Aparicio. "Location, location, location: it's all in the timing for replication origins". In: *Genes & Development* 27.2 (Jan. 15, 2013), pp. 117–128. ISSN: 0890-9369. DOI: 10.1101/gad.209999.112.

[29] Claire Renard-Guillet et al. "Temporal and spatial regulation of eukaryotic DNA replication: From regulated initiation to genome-scale timing program". In: *Seminars in Cell & Developmental Biology* 30 (June 2014), pp. 110–120. ISSN: 10849521. DOI: 10.1016/j.semcdb.2014.04.014.

[30] Mirit I. Aladjem and Christophe E. Redon. "Order from clutter: selective interactions at mammalian replication origins". In: *Nature Reviews Genetics* 18.2 (Feb. 2017), pp. 101–116. ISSN: 1471-0056, 1471-0064. DOI: 10.1038/nrg.2016.141.

[31] Marcel Méchali et al. "Genetic and epigenetic determinants of DNA replication origins, position and activation". In: *Current Opinion in Genetics & Development* 23.2 (Apr. 2013), pp. 124–131. ISSN: 0959437X. DOI: 10.1016/j.gde.2013.02.010.

[32] Benjamin D. Pope and David M. Gilbert. "The Replication Domain Model: Regulating Replicon Firing in the Context of Large-Scale Chromosome Architecture". In: *Journal of Molecular Biology* 425.23 (Nov. 2013), pp. 4690–4695. ISSN: 00222836. DOI: 10.1016/j.jmb.2013.04.014.

[33] N. Rhind and D. M. Gilbert. "DNA Replication Timing". In: *Cold Spring Harbor Perspectives in Biology* 5.8 (Aug. 1, 2013), a010132–a010132. ISSN: 1943-0264. DOI: 10.1101/cshperspect.a010132.

[34] E. Lieberman-Aiden et al. "Comprehensive Mapping of Long-Range Interactions Reveals Folding Principles of the Human Genome". In: *Science* 326.5950 (Oct. 9, 2009), pp. 289–293. ISSN: 0036-8075, 1095-9203. DOI: 10.1126/science.1181369.

[35] Job Dekker, Marc A. Marti-Renom, and Leonid A. Mirny. "Exploring the three-dimensional organization of genomes: interpreting chromatin interaction data". In: *Nature Reviews Genetics* 14.6 (June 2013), pp. 390–403. ISSN: 1471-0056, 1471-0064. DOI: 10.1038/nrg3454.

[36] Boyan Bonev and Giacomo Cavalli. "Organization and function of the 3D genome". In: *Nature Reviews Genetics* 17.11 (Nov. 2016), pp. 661–678. ISSN: 1471-0056, 1471-0064. DOI: 10.1038/nrg.2016.112.

[37] Benoit Moindrot et al. "3D chromatin conformation correlates with replication timing and is conserved in resting cells". In: *Nucleic Acids Research* 40.19 (Oct. 2012), pp. 9470–9481. ISSN: 1362-4962, 0305-1048. DOI: 10.1093/nar/gks736.

[38] T. Ryba et al. "Evolutionarily conserved replication timing profiles predict long-range chromatin interactions and distinguish closely related cell types". In: *Genome Research* 20.6 (June 1, 2010), pp. 761–770. ISSN: 1088-9051. DOI: 10.1101/gr.099655.109.

[39] Jesse R. Dixon et al. "Topological domains in mammalian genomes identified by analysis of chromatin interactions". In: *Nature* 485.7398 (Apr. 11, 2012), pp. 376–380. ISSN: 0028-0836, 1476-4687. DOI: 10.1038/nature11082.

[40] Eitan Yaffe et al. "Comparative Analysis of DNA Replication Timing Reveals Conserved Large-Scale Chromosomal Architecture". In: *PLoS Genetics* 6.7 (July 1, 2010). Ed. by Wendy A. Bickmore, e1001011. ISSN: 1553-7404. DOI: 10.1371/journal.pgen.1001011.

[41] Benjamin D. Pope et al. "Topologically associating domains are stable units of replication-timing regulation". In: *Nature* 515.7527 (Nov. 2014), pp. 402–405. ISSN: 0028-0836, 1476-4687. DOI: 10.1038/nature13986.

[42] Zhijun Duan et al. "A three-dimensional model of the yeast genome". In: *Nature* 465.7296 (May 2010), pp. 363–367. ISSN: 0028-0836, 1476-4687. DOI: 10.1038/nature08973.

[43] T. Pichugina et al. "A diffusion model for the coordination of DNA replication in Schizosaccharomyces pombe". In: *Scientific Reports* 6.1 (May 2016). ISSN: 2045-2322. DOI: 10.1038/srep18757.

[44] Arach Goldar et al. "A Dynamic Stochastic Model for DNA Replication Initiation in Early Embryos". In: *PLoS ONE* 3.8 (Aug. 6, 2008). Ed. by Nick Rhind, e2919. ISSN: 1932-6203. DOI: 10.1371/journal.pone.0002919.

[45] Olivier Hyrien and Arach Goldar. "Mathematical modelling of eukaryotic DNA replication". In: *Chromosome Research* 18.1 (Jan. 2010), pp. 147–161. ISSN: 0967-3849, 1573-6849. DOI: 10.1007/s10577-009-9092-4.

[46] Michel G. Gauthier and John Bechhoefer. "Control of DNA Replication by Anomalous Reaction-Diffusion Kinetics". In: *Physical Review Letters* 102.15 (Apr. 16, 2009). ISSN: 0031-9007, 1079-7114. DOI: 10.1103/PhysRevLett.102.158104.

[47] Michel G. Gauthier, Paolo Norio, and John Bechhoefer. "Modeling Inhomogeneous DNA Replication Kinetics". In: *PLoS ONE* 7.3 (Mar. 7, 2012). Ed. by Jerome Mathe, e32053. ISSN: 1932-6203. DOI: 10.1371/journal.pone.0032053.

[48] Alessandro P. S. de Moura et al. "Mathematical modelling of whole chromosome replication". In: *Nucleic Acids Research* 38.17 (Sept. 2010), pp. 5623–5633. ISSN: 1362-4962, 0305-1048. DOI: 10.1093/nar/gkq343.

[49] Renata Retkute, Conrad A. Nieduszynski, and Alessandro de Moura. "Dynamics of DNA Replication in Yeast". In: *Physical Review Letters* 107.6 (Aug. 4, 2011). ISSN: 0031-9007, 1079-7114. DOI: 10.1103/PhysRevLett.107.068103.

[50] Y. Gindin et al. "A chromatin structure-based model accurately predicts DNA replication timing in human cells". In: *Molecular Systems Biology* 10.3 (Mar. 28, 2014), pp. 722–722. ISSN: 1744-4292. DOI: 10.1002/msb.134859.

[51] J. Lygeros et al. "Stochastic hybrid modeling of DNA replication across a complete genome". In: *Proceedings of the National Academy of Sciences* 105.34 (Aug. 26, 2008), pp. 12295–12300. ISSN: 0027-8424, 1091-6490. DOI: 10.1073/pnas.0805549105.

[52] Konstantinos Koutroumpas and John Lygeros. "Modeling and analysis of DNA replication". In: *Automatica* 47.6 (June 2011), pp. 1156–1164. ISSN: 00051098. DOI: 10.1016/j.automatica.2011.02.007.

[53] D. Löb et al. "3D replicon distributions arise from stochastic initiation and domino-like DNA replication progression". In: *Nature Communications* 7.1 (Dec. 2016). ISSN: 2041-1723. DOI: 10.1038/ncomms11207.

[54] Jean-Michel Arbona et al. "The eukaryotic bell-shaped temporal rate of DNA replication origin firing emanates from a balance between origin activation and passivation". In: *eLife* 7 (June 1, 2018). ISSN: 2050-084X. DOI: 10.7554/eLife.35192.

[55] John Bechhoefer and Brandon Marshall. "How Xenopus Laevis Replicates DNA Reliably even though Its Origins of Replication are Located and Initiated Stochastically". In: *Physical Review Letters* 98.9 (Feb. 27, 2007). ISSN: 0031-9007, 1079-7114. DOI: 10.1103/PhysRevLett.98.098105.

[56] Arach Goldar, Marie-Claude Marsolier-Kergoat, and Olivier Hyrien. "Universal Temporal Profile of Replication Origin Activation in Eukaryotes". In: *PLoS ONE* 4.6 (June 12, 2009). Ed. by Jürg Bähler, e5899. ISSN: 1932-6203. DOI: 10.1371/journal.pone.0005899.

[57] Ralph S. Grand et al. "Chromosome conformation maps in fission yeast reveal cell cycle dependent sub nuclear structure". In: *Nucleic Acids Research* 42.20 (Nov. 10, 2014), pp. 12585–12599. ISSN: 1362-4962, 0305-1048. DOI: 10.1093/nar/gku965.

[58] Takeshi Mizuguchi, Jemima Barrowman, and Shiv I.S. Grewal. "Chromosome domain architecture and dynamic organization of the fission yeast genome". In: *FEBS Letters* 589.20 (Oct. 7, 2015), pp. 2975–2986. ISSN: 00145793. DOI: 10.1016/j.febslet.2015.06.008.

[59] H. Funabiki. "Cell cycle-dependent specific positioning and clustering of centromeres and telomeres in fission yeast". In: *The Journal of Cell Biology* 121.5 (June 1, 1993), pp. 961–976. ISSN: 0021-9525, 1540-8140. DOI: 10.1083/jcb.121.5.961.

[60] Eugenio Cinquemani et al. "Numerical analysis of FRAP experiments for DNA replication and repair". In: *2008 47th IEEE Conference on Decision and Control*. 2008 47th IEEE Conference on Decision and Control. Cancun, Mexico: IEEE, 2008, pp. 155–160. ISBN: 978-1-4244-3123-6. DOI: 10.1109/CDC.2008.4738718.

[61] Maria Anna Rapsomaniki et al. "Inference of protein kinetics by stochastic modeling and simulation of fluorescence recovery after photobleaching experiments". In: *Bioinformatics* 31.3 (Feb. 1, 2015), pp. 355–362. ISSN: 1460-2059, 1367-4803. DOI: 10.1093/bioinformatics/btu619.

[62] Harold J Kushner et al. *Numerical Methods for Stochastic Control Problems in Continuous Time*. OCLC: 1066186723. New York, NY: Springer, 2013. ISBN: 978-1-4613-0007-6.

[63] Atanas Kaykov and Paul Nurse. "The spatial and temporal organization of origin firing during the S-phase of fission yeast". In: *Genome Research* 25.3 (Mar. 2015), pp. 391–401. ISSN: 1088-9051, 1549-5469. DOI: 10.1101/gr.180372.114.

[64] Franziska Bleichert, Michael R. Botchan, and James M. Berger. "Crystal structure of the eukaryotic origin recognition complex". In: *Nature* 519.7543 (Mar. 2015), pp. 321–326. ISSN: 0028-0836, 1476-4687. DOI: 10.1038/nature14239.

[65] Ningning Li et al. "Structure of the eukaryotic MCM complex at 3.8 Å". In: *Nature* 524.7564 (Aug. 2015), pp. 186–191. ISSN: 0028-0836, 1476-4687. DOI: 10.1038/nature14685.

[66] J.M. Mitchison and J. Creanor. "Further measurements of DNA synthesis and enzyme potential during cell cycle of fission yeast Schizosaccharomyces pombe". In: *Experimental Cell Research* 69.1 (Nov. 1971), pp. 244–247. ISSN: 00144827. DOI: 10.1016/0014-4827(71)90337-5.

[67] John Herrick et al. "Kinetic Model of DNA Replication in Eukaryotic Organisms". In: *Journal of Molecular Biology* 320.4 (July 2002), pp. 741–750. ISSN: 00222836. DOI: 10.1016/S0022-2836(02)00522-3.

[68] Prasanta K. Patel et al. "The Hsk1(Cdc7) Replication Kinase Regulates Origin Efficiency". In: *Molecular Biology of the Cell* 19.12 (Dec. 2008). Ed. by Daniel J. Lew, pp. 5550–5558. ISSN: 1059-1524, 1939-4586. DOI: 10.1091/mbc.e08-06-0645.

[69] Davide Mantiero et al. "Limiting replication initiation factors execute the temporal programme of origin firing in budding yeast: Limiting replication factors execute temporal programme". In: *The EMBO Journal* 30.23 (Nov. 30, 2011), pp. 4805–4814. ISSN: 02614189. DOI: 10.1038/emboj.2011.404.

[70] Pei-Yun Jenny Wu and Paul Nurse. "Establishing the Program of Origin Firing during S Phase in Fission Yeast". In: *Cell* 136.5 (Mar. 2009), pp. 852–864. ISSN: 00928674. DOI: 10.1016/j.cell.2009.01.017.

[71] Seiji Tanaka et al. "Origin Association of Sld3, Sld7, and Cdc45 Proteins Is a Key Step for Determination of Origin-Firing Timing". In: *Current Biology* 21.24 (Dec. 2011), pp. 2055–2063. ISSN: 09609822. DOI: 10.1016/j.cub.2011.11.038.

[72] Olivier Hyrien, Kathrin Marheineke, and Arach Goldar. "Paradoxes of eukaryotic DNA replication: MCM proteins and the random completion problem". In: *BioEssays* 25.2 (Feb. 2003), pp. 116–125. ISSN: 02659247, 15211878. DOI: 10.1002/bies.10208.